

Efects of magnetic and non-magnetic impurities on the Superconducting State of $\text{YBa}_2\text{Cu}_3\text{O}_7$

M. Le Tacon,^{1,2} A. Sacuto,^{1,2} Y. Gallais,³ E. Sherman,⁴ and D. Colson⁵

¹Laboratoire Matériaux et phénomènes Quantiques (UMR 7162 CNRS), Université Paris 7, 2 place Jussieu 75251 Paris, France

²Laboratoire de Physique du Solide ESPCI, 10 rue Vauquelin 75231 Paris, France

³Departments of Physics and Applied Physics, Columbia University New York, NY 10027, USA

⁴Institut für Theoretische Physik, University Graz, Universitätsplatz 5, A-8010 Graz, Austria

⁵Service de Physique de l'Etat Condensé, CEA-Saclay, 91191 Gif-sur-Yvette, France

(Dated: May 24, 2019)

We report Electronic Raman Scattering measurements on optimally doped Zn and Ni substituted YBCO in A_{1g} and B_{1g} channels. We show that the superconducting gap energy is independent of magnetic Ni and non-magnetic Zn substitutions. On the contrary the collective A_{1g} mode follows the critical temperature T_c with two distinct slopes for Ni and Zn, and tracks the magnetic resonance seen in inelastic neutron scattering. We explain the unconventional energy dependence of the superconducting gap and discuss the behaviour of the A_{1g} mode within magnetic and non-magnetic impurities.

PACS numbers: 74.62.Dh, 74.72.-h, 78.30.-j

In the last few years, transport [1], nuclear magnetic resonance (NMR) [2], muon spin relaxation (μ -SR) [3, 4] and scanning tunneling microscopy (STM) [5] measurements have shown that the effect of non-magnetic impurities was much more drastic than the effect of magnetic ones, and therefore can be used as a relevant probe for testing the quasiparticles and the collective modes in the superconducting state. Raman Scattering is a powerful tool for probing electronic excitations in selected areas of the cuprate's Fermi surface. Raman responses are very sensitive to the d-wave character of the superconducting gap (SG). The B_{1g} channel [6] probes the antinodal regions where the SG amplitude is maximum and the B_{2g} channel [6] probes the nodal regions where the SG vanishes. The A_{1g} channel [6] has no symmetry restriction and is sensitive to nodal and antinodal regions of the Fermi surface. In the A_{1g} channel a strongly Raman active collective mode (the " A_{1g} mode"), which origin is not yet identified, is definitively observed in the superconducting state of optimally doped cuprates [7], below 2 energy. It has been shown that the A_{1g} mode, tracks the acoustic part of the magnetic resonance detected by inelastic neutron scattering (INS) [8] at $Q_{AF} = (1, 0)$ for both its temperature and energy dependence within magnetic Ni substitutions. In this letter we report the effects of non-magnetic Zn substitutions on the electronic Raman responses in A_{1g} and B_{1g} channels of optimally doped YBCO and check them with the effect of magnetic Ni substitutions. We show that the 2 amplitude of the SG remains constant under magnetic or non-magnetic impurity substitutions up to 3%, and the energy of the A_{1g} mode follows T_c with two distinct slopes for magnetic and non-magnetic substitutions, as the magnetic resonance energy.

Using an intermediate limit scattering potential with

anisotropic phase shift for Ni impurities and an unitary limit scattering in the "Swiss Cheese" [3] model for Zn impurities, we explain the unexpected SG energy dependence and discuss the A_{1g} collective mode behaviour.

In addition to the pure $\text{YBa}_2\text{Cu}_3\text{O}_7$ ($\text{Y}-123$, $T_c = 92.5\text{K}$), we have studied $\text{YBa}_2(\text{Cu}_{1-y}\text{Zn}_y)_3\text{O}_7$ single crystals with $y = 0.005$ ($T_c = 87.5\text{K}$), $y = 0.01$ ($T_c = 83\text{K}$), $y = 0.02$ ($T_c = 73\text{K}$) and $y = 0.03$ ($T_c = 64\text{K}$). These crystals have been renamed $\text{Y}-123$, $\text{Y}-123\text{Zn87K}$, $\text{Y}-123\text{Zn83K}$, $\text{Y}-123\text{Zn73K}$ and $\text{Y}-123\text{Zn64K}$ respectively and the Ni substituted crystals of [8], $\text{Y}-123\text{Ni87K}$ and $\text{Y}-123\text{Ni78K}$.

YBCO systems are optimally doped single crystals grown by the "self-flux" method [9]. Zn is a divalent ion known to substitute preferentially in the copper oxygen planes of YBCO, without changing the carrier concentrations [10]. Impurity concentrations were checked by chemical analysis using an electron probe, and the critical temperature of each crystals has been determined by DC-squid magnetization measurements. Raman measurements have been performed on a T64000 JY spectrometer in triple subtractive configuration. YBCO single crystals were xed on the cold finger of an He circulation cryostat that cools down to 10 K. The 514 nm excitation line of a (Ar^+ , Kr^+) laser was used. The laser spot was about 100 μm of diameter and the power on the crystal surface was kept below 3 mW to avoid heating (that was not bigger than 3 K according to Stokes-Anti-Stokes measurements.). After correction of the raw spectra from the Bose factor $n(\omega; T)$, we obtain the imaginary part of the Raman susceptibility $\Im(\omega) = I(\omega) = [1 + n(\omega; T)]$ [11].

$\Im(\omega)$ in normal and superconducting states in the A_{1g} (resp. B_{1g}) channel for various Zn concentrations are shown in the left (resp. right) panel of Figure 1. For pure YBCO (on the top of Figure 1), we have a clear

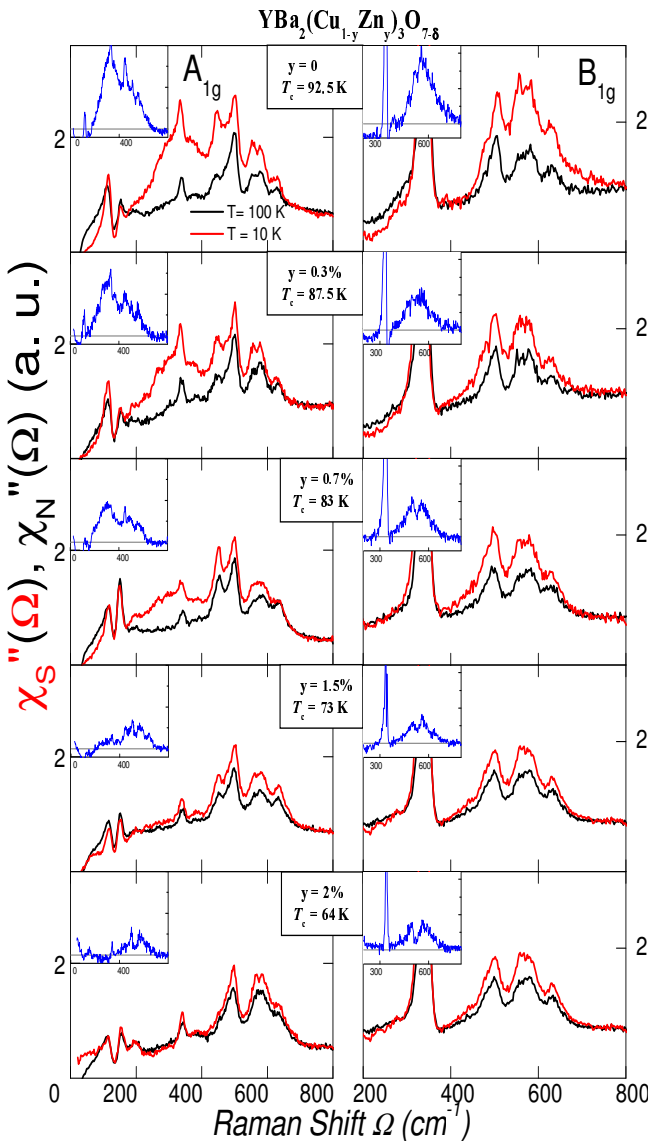


FIG. 1: Superconducting and normal Raman responses $\chi_s''(\Omega)$ and $\chi_n''(\Omega)$ for optimally doped $\text{YBa}_2(\text{Cu}_{1-y}\text{Zn}_y)_3\text{O}_7$ crystals. The difference $\chi_s''(\Omega) - \chi_n''(\Omega)$ is plotted in the inset. Spectra have been normalised to $\chi_0''(\Omega)$, where $\chi_0''(\Omega)$ is the crossover between normal and superconducting Raman responses ($\chi_0^{A_{1g}} = 170 \text{ cm}^{-1}$ response and $\chi_0^{B_{1g}} = 400 \text{ cm}^{-1}$).

enhancement of the A_{1g} and B_{1g} electronic responses between (170 – 670 cm^{-1}) and (400 – 800 cm^{-1}) respectively in the superconducting state with respect to the normal state. Subtraction of the normal contribution from the superconducting one are shown in insets of Figure 1. As a result in B_{1g} channel, we obtain well defined peak centered at 565 cm^{-1} ($8.8 k_B T_c$) corresponding to the 2 pair breaking energy of the SG [12]. In the A_{1g} channel, for pure YBCO , the subtraction gives rise to a broad asymmetric peak, in which two distinct contributions have been already established [7]. The first one is the A_{1g} collective mode centered on 331 cm^{-1} ($5 k_B T_c$), that runs from 170 to 410 cm^{-1} and the second one, from 410 to 670 cm^{-1} is the SG signature in the A_{1g} channel [7].

As Zn concentration increases, the A_{1g} mode broadens, shifts to lower energies and decreases in intensity. In $\text{Y}-123\text{Zn}73\text{K}$, a weak contribution of the A_{1g} mode subsists, while in $\text{Y}-123\text{Zn}64\text{K}$, it disappears. On the other hand, the SG energy remains constant with Zn substitutions, at the contrary to what is assumed in Ref.[13]. Its intensity also falls down, but in $\text{Y}-123\text{Zn}64\text{K}$ a weak SG response is still there in agreement with the B_{1g} response.

In Figure 2 are reported the A_{1g} mode and SG energies with respect to T_c for Ni and Zn substituted YBCO . In both cases, the SG positions remain constant as the impurity concentrations increase: we find that the mean value of the B_{1g} peak is $\langle \omega \rangle = 67.6 \text{ meV}$ (2.5 meV). It has already been shown that changes of T_c under oxygen doping fail to keep the $\omega = k_B T_c$ ratio constant as expected in BCS theory. Our data show that even for fixed doping (here the optimal one), when T_c decreases under magnetic (see [8]) or non-magnetic impurities substitutions, $\omega = k_B T_c$ is not constant anymore. The energy of the A_{1g} mode follows $5k_B T_c$ in the Ni case, whereas for Zn it follows $k_B (2.2T_c + 2.8T_c^{\text{opt}})$, where $T_c^{\text{opt}} = 92.5 \text{ K}$ is the optimal T_c of Zn-free YBCO ($\text{Y}-123$).

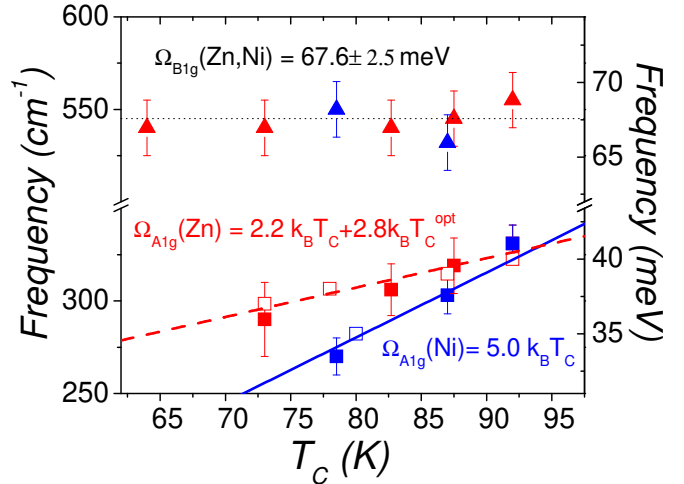


FIG. 2: Energies of the SG peak (filled triangles), A_{1g} mode (filled squares) and of the neutron resonance (empty squares) with respect to T_c under magnetic Ni (gray) and non-magnetic Zn (black) impurity substitutions.

STM measurements on local electronic structure of cuprates under magnetic Ni substitutions have shown that the quasiparticle scattering on impurities was predominantly potential, rather than magnetic [14]. From this statement, we have calculated the superconducting density of states (SDOS) for a CuO_2 plane where Cu is substituted by Ni. Considering potential pair breaking in a d-wave model, described by the Matsubara Green functions $G(\mathbf{k}; i\omega_n) = \frac{i\omega_n + \frac{\pi}{k}}{(i\omega_n)^2 - \frac{\pi^2}{k^2}}$, $i\omega_n = i\omega_n - (i\omega_n)$. The SDOS is given by:

$$N_S(E) = \frac{1}{2\pi} \sum_{\mathbf{k}} \frac{X}{(i\omega_n)^2 - \frac{\pi^2}{k^2}} G(\mathbf{k}; i\omega_n) i\omega_n - E + i0^+ \quad (1)$$

Scattering in the Born ($\gamma = 0$) and unitary limit ($\gamma = \pi/2$) have already been treated in previous work [15]. The scattering on Ni impurities has been found to be located between these two limits [14], therefore we have chosen an intermediate phase shift for potential impurity scattering. Furthermore, due to the anisotropy of the Fermi velocity v_F in cuprates, we have chosen an anisotropic phase shift (γ). This is taken into account in the self-energy $(i!_n)$ [16]:

$$(i!_n) = \frac{n_{\text{imp}}}{(N_F)^2} \frac{k_p \tan(\gamma(k))}{[k \tan(\gamma(k))G(k;i!_n)]^2} \quad (2)$$

where n_{imp} stands for Ni impurity concentration, and N_F for the DOS at the Fermi level in the normal state.

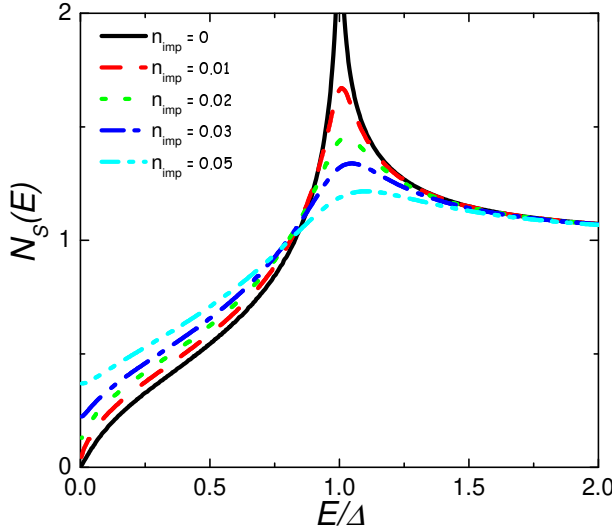


FIG. 3: Evolution of the SD DOS for a d-wave superconductor within potential scatterers concentration.

In figure 3, we have plotted the SD DOS as a function of energy E for different n_{imp} (up to 5%). At $E = 0$, with no impurities, the DOS diverges. As Ni impurities are inserted, the DOS exhibits a maximum at the same energy and a finite DOS at $E = 0$ that increases with n_{imp} . Low energy excitations in the superconducting state come from quasiparticles of the nodal regions. $N(E = 0)$ growing up when n_{imp} increases means that superconductivity is destroyed around the nodes of the SG, where the interaction leading to the Cooper pairs formation is weaker. This is consistent with B_{2g} Raman data [17] which reveals no distinctions between superconducting and normal B_{2g} responses already at 1% of Ni impurities. This explains also why the B_{2g} response is more generally affected by any scattering source (e.g. structural disorder) as previously observed [17, 18, 19]. The SD DOS maximum remaining at $E = 0$ as n_{imp} increases, the quasiparticles in the antinodal regions are not affected, and thus no changes are seen in the energy of the B_{1g} peak. However, $N_s(E = 0)$ of the DOS decreases as n_{imp} increases, which implies the decrease of the B_{1g} peak intensity as observed experimentally [8].

The situation is different for non-magnetic impurities since the scattering has been found to be almost unitary ($\gamma = 0.48 \pi$). As a consequence, the superconducting order parameter is suppressed locally around each impurity site, and the superfluid density decreases. This gives rise to the "Swiss Cheese" model and explains why the SG intensity decreases as Zn concentration increases. To achieve the calculation of the DOS in a Zn substituted cuprate, one must thus take into account spatial inhomogeneities of the superconducting order parameter, making the calculation more complicated. However, our data suggest that, in the remaining superconducting condensate, the Cooper pairs binding energy is not altered, and thus no changes are seen in the pair breaking peak in the B_{1g} channel. At this step, it is interesting to notice that non-magnetic impurities effects, at least on transport and T_c , can be reproduced by defects induced by electron irradiation [1] in cuprates. Angle resolved photoemission spectroscopy (ARPES) measurements performed on such irradiated samples (Bi2212 with a T_c down to 62 K) have revealed no changes in the SG energy with respect to T_c [20]. This is consistent with our data.

In Figure 2, we have added to the A_{1g} modes energies under Ni and Zn substitutions, the magnetic resonance energies obtained from [21, 22]. This shows unambiguously that for Ni and Zn substitutions, the A_{1g} mode tracks the magnetic resonance. As a consequence, magnetic and non-magnetic impurities lead to two different slopes for both the A_{1g} mode and the magnetic resonance.

To go further, we have plotted in Figure 4 the temperature dependences of the A_{1g} mode for four crystals Y-123, Y-123:Zn83K, Y-123:Ni87K and Y-123:Ni78K.

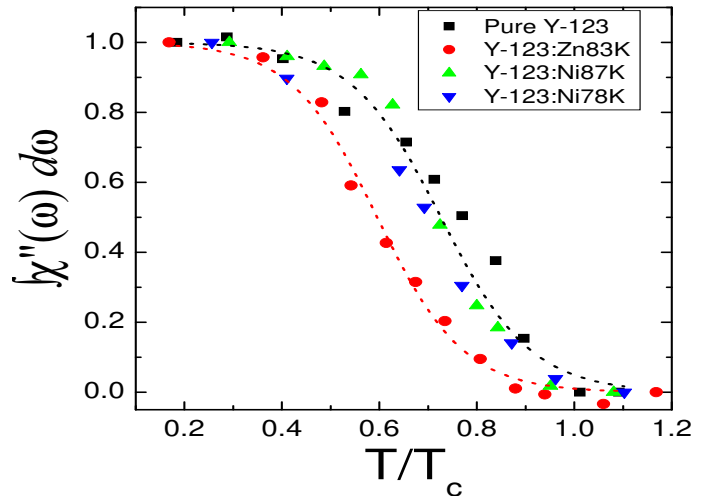


FIG. 4: Temperature dependences of the spectral weight between 170 cm^{-1} and 420 cm^{-1} of the A_{1g} mode. The temperature scale has been normalized to T_c for each crystal.

We clearly see that the A_{1g} mode starts growing just below T_c in Ni-substituted YBCO, in the same way as pure YBCO. On the contrary, in the Zn case the A_{1g} mode exhibits a temperature delay of ($0.8 k_B T_c - 20 \text{ K}$)

In the Ni case, the A_{1g} mode spectral weight follows the one of the free YBCO as function of temperature. The energies of both A_{1g} mode and magnetic resonance follow $5 k_B T_c$ for Ni-substituted and pure YBCO (Figure 2), and STM measurements have shown the presence of localised states on the Ni impurity, but no disruption of superconductivity near impurity [14]. These three experimental observations suggest that superconductivity is homogeneously modified by the introduction of magnetic impurities, and that the mechanism that leads to the formation of both magnetic resonance and A_{1g} mode is not fundamentally altered, but rather renormalised with respect to T_c . The scenario is different in the Zn case. On one hand, the shifts in energy for both the A_{1g} mode and magnetic resonance is smaller than in the case of magnetic substitutions (Figure 2). On the other hand, we see (Figure 1) that the intensity of the A_{1g} mode decreases strongly with increasing Zn concentration, and for a concentration greater than 2% this mode disappears, in contrast with the Ni case [8]. Finally, Figure 4 shows that the A_{1g} mode starts growing 20 K below T_c in the Y-123:Zn83K crystal. Consequently, under non-magnetic substitutions it exists Zn concentrations where superconductivity is there, but where the A_{1g} mode is not yet present. This brings us to conclude that the diminution of superuid density observed in -SR [3, 4] for Zn-substituted samples do not explain alone the disappearance of the A_{1g} mode. As it has been shown previously, AF fluctuations at $Q_{AF} = (1/2, 1/2)$ are strongly enhanced above T_c in Zn-substituted samples [22], and survive in the superconducting state. We think that these fluctuations put back the A_{1g} mode and the neutron resonance [22], and that the disappearance of these two collective modes when Zn concentration is larger than 2% results from a conjugate effect of AF fluctuations and of the diminution of the superuid density.

In conclusion, we have shown that the unconventional behaviour of the superconducting gap can be explained under a simple potential scattering model for Ni magnetic substitutions. Through Zn non-magnetic substitutions, we have confirmed the strong link between the magnetic resonance and the A_{1g} mode. The A_{1g} mode in Zn substituted YBCO exhibits a significant temperature delay from T_c in comparison to the one in the Ni substituted YBCO due to the presence of strong antiferromagnetic fluctuations.

Acknowledgements: We thank S. Pailles, Y. Sidis, Ph. Bourges, M. Cazayous, K. Behnia, and P. Monod for very fruitful discussions.

- [1] F. Rullier-Albenque, P.A. Viallet, H. Aloul, A.W. Tyler, P. Lejay, and J.F. Marucco, Phys. Rev. Lett. 91, 047001 (2003).
- [2] J. Bobro, W.A. MacFarlane, H. Aloul, P.M. Endels, N. Blanchard, G. Collin, and J.F. Marucco, Phys. Rev. Lett. 83, 4381 (1999).
- [3] B. Nachumi, A. Keren, K. Kojima, M. Larkin, G.M. Luke, J. Merrin, O. Tchernyshov, Y.J. Uemura, N. Ichikawa, M. Goto, and S. Uchida, Phys. Rev. Lett. 77, 5421 (1996).
- [4] C. Bernhard, J.L. Tallon, C. Bucci, R. De Renzi, G. Guidi, G.V.M. Williams, and Ch. Niedermayer, Phys. Rev. Lett. 77, 2304 (1996).
- [5] S.H. Pan, E.W. Hudson, K.M. Lang, H. Eisaki, S. Uchida, and J.C. Davis, Nature 403, 746 (2000).
- [6] B_{2g} and B_{1g} channels are obtained from cross polarizations of the incident and scattered electric fields along and at 45 degrees from the Cu-O bounds of CuO₂ layers. Parallel polarizations at 45 degrees from the Cu-O bounds give the $A_{1g} + B_{2g}$ channel, and pure A_{1g} channel is obtained by subtracting the B_{2g} one from the $A_{1g} + B_{2g}$ one.
- [7] M. Le Tacon, A. Sacuto, and D. Colson, Phys. Rev. B 71, R100504 (2005).
- [8] Y. Gallais, A. Sacuto, P. Bourges, Y. Sidis, A. Forget, and D. Colson, Phys. Rev. Lett. 88, 177401 (2002).
- [9] D.L. Kaiser, F. Holtzberg, B.A. Scott, and T.R. McGuire, Appl. Phys. Lett. 51, 1040 (1987).
- [10] A.V.M. Ahajan, H. Aloul, G. Collin, and J.F. Marucco, Phys. Rev. Lett. 72, 3100 (1994); J. Bobro, H. Aloul, P. M. Endels, V. Viallet, J.F. Marucco, and D. Colson, Phys. Rev. Lett. 78, 3757 (1997).
- [11] A. Sacuto, J. Cayssol, D. Colson, and P. Monod, Phys. Rev. B 61, 7122 (2000).
- [12] N.M. Miyakawa, P. Guptasarma, J.F. Zasadzinski, D.G. Hinks, and K.E. Gray, Phys. Rev. Lett. 80, 157 (1998).
- [13] H. Martinho, A.A.M. Martin, C. Rettori, and C.T. Lin, Phys. Rev. B 69, 180501 (2004).
- [14] E.W. Hudson, K.M. Lang, V.M. Adhavan, S.H. Pan, H. Eisaki, S. Uchida, and J.C. Davis, Nature 411, 920 (2001).
- [15] L.S. Borkowski and P.J. Hirschfeld, Phys. Rev. B 49, R15404 (1994); R. Fehrenbacher and M.R. Norman, Phys. Rev. B 50, R3495 (1994).
- [16] V.P. Mineev and K.V. Samokhin, Introduction to Unconventional Superconductivity, Gordon and Breach, Amsterdam (1999); J.-M. Tang and M.E. Flatté, Phys. Rev. B 66, R060504 (2002).
- [17] Y. Gallais, Thèse de Doctorat de l'Université Paris VI (2003).
- [18] Y. Gallais, A. Sacuto, T.P. Devreux, and D. Colson, Phys. Rev. B 71 B 012506 (2005).
- [19] R. Nemetschek, M. Opel, C. Homann, P.F. Müller, R. Hackl, H. Berger, L. Forro, A. Erb, and E.W. Walker, Phys. Rev. Lett. 78, 4837 (1997).
- [20] I. Voborník, H. Berger, D. Pavuna, M. Onellion, G.M. Margaritondo, F. Rullier-Albenque, L. Forro, and M. G. Rionti, Phys. Rev. Lett. 82, 3128 (1999).
- [21] Y. Sidis, P. Bourges, H.F. Fong, B. Keimer, L.P. Regnault, J. Bossy, A. Ivanov, B. Hennion, P. Gauthier-Picard, G. Collin, D.L. Milius, and Ia. Aksay, Phys. Rev. Lett. 84, 5900 (2000);
- [22] Y. Sidis, P. Bourges, B. Hennion, L.P. Regnault, R. Villeneuve, G. Collin, and J.F. Marucco, Phys. Rev. B 53, 6811 (1996); Y. Sidis, P. Bourges, B. Keimer, L.P. Regnault, J. Bossy, A. Ivanov, B. Hennion, P. Gauthier-Picard, and G. Collin, Condmat 0006265.